APPLICATION OF COMPUTATIONAL AERODYNAMICS METHODS TO THE DESIGN AND ANALYSIS OF TRANSPORT AIRCRAFT

A. Larry da Costa
Boeing Commercial Airplane Company
Seattle, Washington

Abstract

The application and validation of several computational aerodynamic methods in the design and analysis of transport aircraft is established. An assessment is made concerning more recently developed methods that solve three-dimensional transonic flow and boundary layers on wings.

Capabilities of subsonic aerodynamic methods are demonstrated by several design and analysis efforts. Among the examples cited are the B747 Space Shuttle Carrier Aircraft analysis, nacelle integration for transport aircraft, and winglet optimization. The accuracy and applicability of a new three-dimensional viscous transonic method is demonstrated by comparison of computed results to experimental data.

I. Introduction

The present state-of-the-art in aerodynamic design requires extensive configuration refinement through repeated wind tunnel testing. This is costly, and time consuming; and it relies heavily on the experience and expertise of the members of the design group. Several key concerns exist regarding this practice: model mounting support systems and wall interference effects cast doubts on the accuracy of wind tunnel results at transonic speeds; limited Reynolds number capability of existing tunnel facilities introduce large risks in extrapolating wind tunnel results to full-scale conditions; and current instrumentation and flow visualization techniques provide only limited knowledge of the flow field around the aircraft. It is becoming clear that these concerns are lessened whenever applicable computational tools, viz., computer programs, are available. Considerable confidence in several of these computational aerodynamic methods has been generated due to their successful application in a wide range of design problems. Consequently, these computational tools are now having a large impact on current design of aircraft configurations. These methods guide the engineer designer in achieving efficient integrated designs, in gaining insight into complex flow fields, and in exploring innovative configuration concepts.

A summary of some of the currently available computational methods are presented, and examples are shown of their application to a variety of aircraft design and analysis problems. Some cases will illustrate how computational methods are able to solve problems that are too difficult or too costly to accomplish by wind tunnel testing. Other cases will show that computational methods can provide a more comprehensive physical description of the flow than can be obtained by testing, and also provide meaningful results for achieving integrated designs.

II. Description of Computational Aerodynamics Methods

A large selection of computational methods are available that have broad application to the analysis and design of transport aircraft flying in the subsonic and transonic speed regimes. A thorough review of these methods will not be given here since the background literature is easily accessible. On the other hand, their main features pertinent to the work presented herein are breifly discussed.

Three-Dimensional Potential Flow Method For Arbitrary Configurations

A computational method has been developed at The Boeing Company that can treat arbitrary three-dimensional potential flows. [1, 2, 3] This is a linear method solving Laplace's equation satisfying exact boundary conditions. In this approach the velocity potential at any point in a flow field is expressed in terms of the induced effects of source and doublet (or vortex) sheets distributed on the boundary surfaces. The configuration surfaces are divided into panels, and hence, this approach has come to be known as a panel method. Essentially, this is a general three-dimensional boundary value problem solver that is capable of being applied to most problems that can be modeled within the limitations of potential flow. Compressibility effects are approximated by the Gothert rule, and thus, analysis of transonic flows is not possible with this method. Viscous effects can be represented by either surface displacement or flow through the surface. This method is ideally suited for analyzing complex aircraft configurations in subsonic flow.

Three-Dimensional Vortex Lattice Method for Arbitrary Configurations

A method based on vortex lattice theory has been developed at The Boeing Company that can be applied to the combined analysis, induced drag optimization, and aerodynamic design of three-dimensional configurations of arbitrary shape. [4] This is a linear method solving Laplace's equation satisfying linearized boundary conditions. Geometric and aerodynamic constraints can be imposed on both the optimization and design processes. Lifting surfaces are represented by multihorseshoe vortex lattices. The design and optimization processes utilize the method of Lagrange multipliers. Although the method assumes incompressible flow, its ease of use, computational speed (low cost), and design capability make it particularly valuable in evaluating design variations, arriving at optimized configurations, and designing new wing camberline shapes.

Trefftz Plane Calculation of Induced Drag

The classical method for estimating lift induced drag for an airplane configuration is by analyzing the trailing vorticity in the wake far downstream, i.e., in the so-called Trefftz plane.[5] The popularity and accuracy of this method has led to its inclusion in other methods, e.g., the vortex lattice method, and to several independent variations. Among the latter is a method which calculates lift and induced drag from sparse loading data.[6] This has proven extremely useful in analyzing wind tunnel data. Another variation of this method features nonplanar geometry capability and an optimization option for computing the load distribution for minimum induced drag subject to force, bending moment, and pitching moment constraints.[7] Since this approach is capable of handling wings with struts and nacelles, it has been used in conjunction with subsonic panel methods that supply load information on each of the configuration components.

Transonic Exhaust Flow Method

The transonic flow field about the aft end of an axisymmetric exhaust nozzle can be calculated by a method that is based on the small disturbance transonic flow equation expressed in cylin-

drical coordinates.[8] Numerical solutions are obtained by finite difference algorithms. This method computes pressure distributions on the internal and external nozzle surfaces, pressure distributions in the flow field, and the shape of the free jet boundary between the external free stream and the exhaust jet. This approach has been used to model the aft end of an engine nacelle including the fan and primary cowls. The resulting plume shapes have been used in connection with three-dimensional potential flow methods to represent the complete nacelle and exhaust plume combination.

Three-Dimensional Transonic Potential Flow Methods

Several three-dimensional transonic potential flow methods have been developed, by various organizations, which are able to analyze either isolated wings or wing-fuselage combinations.[9, 10, 11, 12, 13] Evaluation of these methods indicate that the approach of using finite volume technique to solve the full transonic potential flow equation[10] demonstrates the best agreement between calculated and experimental results. This scheme can be regarded as a finite element method, adapted to treat flows having embedded supersonic regions. It is assumed that any shock waves contained in the flows are weak enough that the entropy and vorticity generated by the shock waves can be neglected. The full potential flow equation is treated in conservation form, i.e., mass is conserved in each element. A shortcoming of the program is that it is unable to treat arbitrary fuselage shapes. Nevertheless, this method is proving to be an extremely valuable tool in analyzing candidate wing designs and complementing test data.

A method based on transonic small disturbance formulation [11] has also demonstrated its usefulness, inasmuch as arbitrary fuselage shapes can be modeled by incorporating analysis provided by subsonic panel methods.[14] This program is currently undergoing further extension to include the capability to handle strut mounted underwing nacelles, and wing-winglet configurations. Unfortunately, the small disturbance assumption is not generally applicable to transport wings, which are relatively thick and characterized by blunt leading edges.

Three-Dimensional Boundary Layer Method

A three-dimensional boundary layer method has been developed at The Boeing Company that can analyze either laminar or turbulent compressible flows on finite swept wings.[15] The method uses an implicit finite difference technique to solve the boundary layer equations. In the turbulent case, a simple eddy viscosity model is used for the turbulent shear stresses. This model can either represent isotropic or nonisotropic eddy viscosity.

The boundary layer method requires that an outer (inviscid) flow description be provided as input. To this end, the three-dimensional transonic potential flow method[10] mentioned above is generally used. An interface program constructs the working boundary layer grid used for the analysis and interpolates the velocity components from the potential flow program into the boundary layer grid. The inclusion of this boundary layer technique into the analysis of future transport aircraft wings not only provides for a better representation of the real flow field for determining wing pressures, but also, enables more accurate drag estimates to be made.

III. Application of Methods

Panel Aerodynamic Methods

Panel aerodynamic methods have been used at The Boeing Company for the past decade. During this time period, the panel method has been validated as a very reliable tool in predicting the aerodynamic characteristics of airplanes operating at subcritical Mach numbers. One of the most impressive examples of its use was on the initial design phase of the B747 Space Shuttle Carrier Aircraft (SCA).[16] The initial design phase was to define the modifications needed to accomplish the following missions: to ferry the Space Shuttle Orbiter; to air-launch the Orbiter; and to ferry the external fuel tank. To keep the cost of the program to a minimum, panel methods were extensively used to investigate the Orbiter attitude during the ferry mission, the Orbiter trajectory and attitude during the launch test, and the external tank location and attitude during its ferry mission. At the conclusion of the design phase, the final selected configurations were tested in the wind tunnel to verify predictions.

A typical example of a paneling scheme of the B747 with the Space Shuttle Orbiter is depicted in Fig. 1. In this example, the Orbiter incidence angle was 8° with respect to the B747 reference plane. The predicted lift coefficient, C_L, as a function of wing angle-of-attack, α_w, for this configuration is shown in Fig. 2. The Mach number, M, is 0.60. The agreement between the analyses and wind tunnel data shown in this figure is excellent.

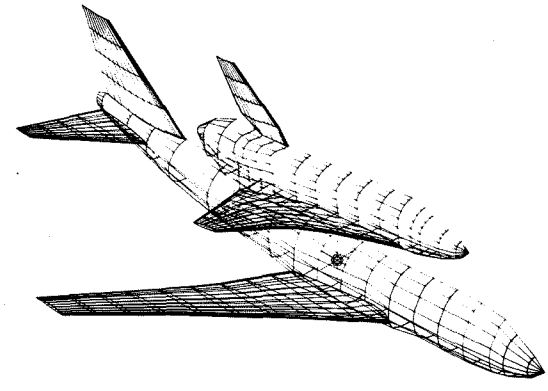

Figure 1 B747 with Space Shuttle Orbiter

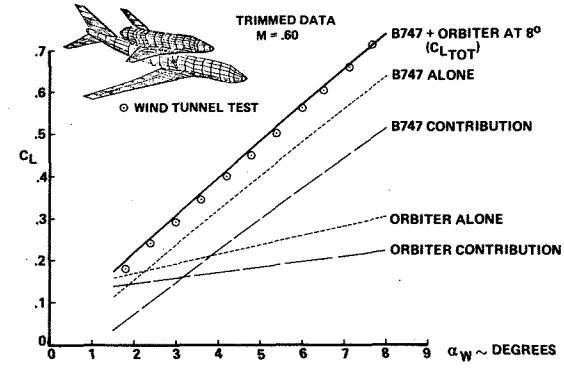

Figure 2 B747-Orbiter Lift Coefficient

The panel methods can be used to calculate the induced drag by integrating the surface pressures of the wing. The mutual interference between the two vehicles (expressed by the difference in induced drag of the combined configuration with respect to the sum of the component parts, $\Delta C_{D_{Installed}}$) as a function of angle-of-attack as predicted using the panel method is portrayed in Fig. 3. This result was later verified by wind tunnel test data.

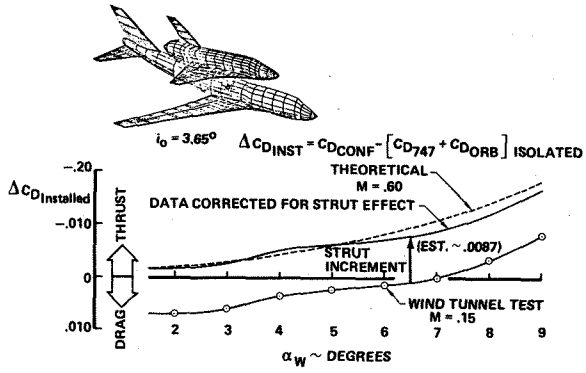

Figure 3 B747-Orbiter Interference Drag Comparison with Wind Tunnel Data

The second mission of the SCA was to provide an air-launch platform for testing the gliding characteristics of the full-scale Orbiter. The B747 wing load distribution during the critical separation maneuver is depicted in Fig. 4. In this figure, η is the fractional semi-span, and thus, $\eta = 0$ denotes the body centerline, and $\eta = 1$ specifies the wing tip.

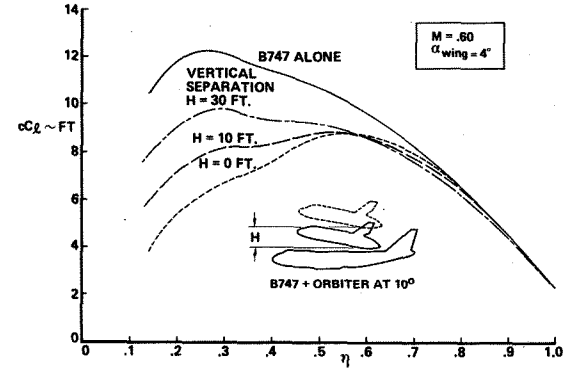

Figure 4 B747 Wing Span Loading During Separation

The third mission requirement was to ferry the external fuel tank of the main booster rocket on top of the B747 SCA from the factory to the launch platform. One of the major concerns with this configuration was its stability along each of three stability axis. The predicted and measured directional stability of the B747 SCA with and without the external tank are shown in Fig. 5. The test data substantiated the predicted trends up to a side slip angle, β, of about 5°. Note that the tank contributes a large destabilizing effect on the total configuration that would have made the configuration unflyable without the addition of vertical fins on the horizontal tail.

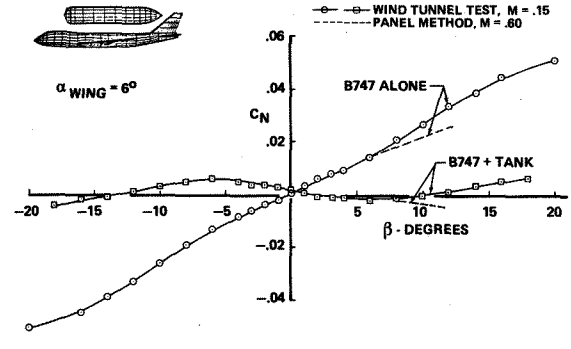

Figure 5 Effect on Tank on B747 Directional Stability

Winglets

Continuing escalating fuel and aircraft operational costs have brought to the forefront the need to improve aircraft cruise efficiency. One of the most attractive concepts to achieve this goal is that of winglets. The possibility to achieve significant performance improvements with these devices has been demonstrated on several transport type configurations.(17, 18, 19) The application of the vortex lattice method, together with the three-dimensional potential flow and induced drag programs provide a powerful analytical capability for the design and analysis of winglet configurations. The procedure and its validation by comparison to wind tunnel results for the B747-200 and KC-135 cruise configurations have been detailed in Reference 20.

The general technique employed in designing winglets is to use the vortex lattice method to calculate the winglet camber and twist to achieve the largest reduction in induced drag at cruise lift. The resulting designed configuration is then analyzed using the panel method. Sample comparisons between measured and predicted pressure distributions for the KC-135 tanker aircraft are shown in Fig. 6. In this figure, ξ is the fractional distance along the winglet. The good correlation shown here has also been obtained on other configurations studied for similar subcritical, unseparated flow conditions. Test-theory comparisons of the KC-135 cruise performance improvements due to winglets are shown in Fig. 7. The percent increase in wing root bending moment, ΔWRBM, as a function of airplane lift coefficient, C_L, is shown at the top of this figure; the predicted and measured increment in drag coefficient, ΔC_D, as a function of C_L is portrayed in the lower left of this figure; and, the improvement in airplane performance in terms of the variation of airplane range factor, M(L/D), with Mach number is depicted at the right of this figure. The agreements are reasonably good and within the accuracy of measured wind tunnel data.

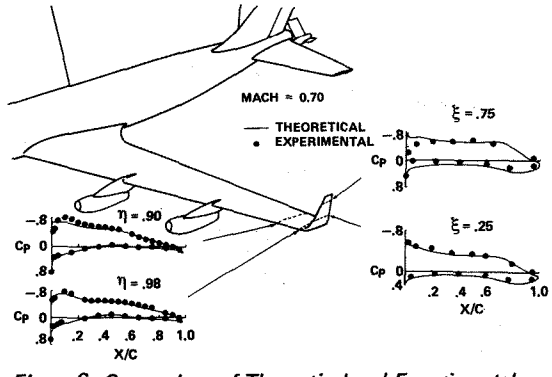

Figure 6 Comparison of Theoretical and Experimental Pressure Distributions - - KC-135 with Winglets

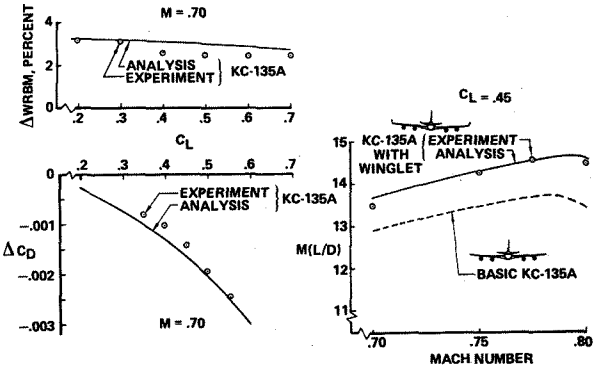

Figure 7 KC-135A Winglet High-speed Performance

Upon achieving a satisfactory winglet design based on cruise conditions, it is possible to further use the three-dimensional potential flow panel method to evaluate the configuration under other operating conditions, e.g., during takeoff and landing. The interest in these cases would be to determine if the winglets caused any adverse low speed characteristics. It has been noted that lift coefficients produced by winglets are proportional to lift coefficients produced by the wing. For modern technology high lift systems, the winglet section lift coefficient, C_{ℓ}, during takeoff and landing could exceed 1.3. Consequently, the winglet flow would separate. Although the computational methods are unable to model separated flows, they are able to suggest the general trend of the configuration performance under such conditions.

An evaluation of the takeoff performance of the KC-135 winglet configuration described in the previous example is shown in Figs. 8 through 11. The panel representation of the configuration studied is shown in Fig. 8. The exterior of the wing, including flaps, were represented by source panels, while the camberline was modeled by multihorsehoe vortices. For a flap setting of $\delta_f = 30°$, corresponding to takeoff conditions, the effect of winglets on the chordwise pressure distribution on the outboard wing are shown in Fig. 9. Evidently, the pressures on the wing were not adversely affected by the winglet. The pressure peaks at the leading edge of the wing were slightly reduced, since winglets cause the outboard wing to carry more lift at a given angle-of-attack. Conversely, the pressure peaks at the leading edge of the winglet are excessive, and significant low speed performance gains could be obtained by incorporating a leading-edge device on the winglet, or by redesigning the winglet to incorporate more leading-edge droop at some cruise drag penalty. A comparison of wind tunnel data to computed winglet pressures is shown in Fig. 10. The agreement is surprisingly good considering that flow separation seems to have occurred on the winglet as evidenced by the level of the pressures at the trailing edge.

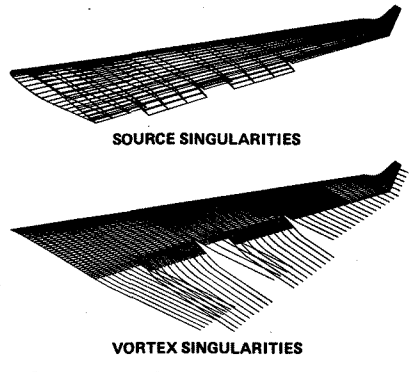

Figure 8 Potential Flow Modeling of Wing and Winglet

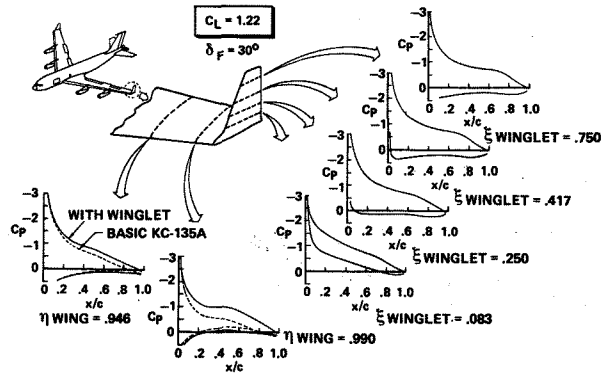

Figure 9 Wing and Winglet Pressures at Takeoff

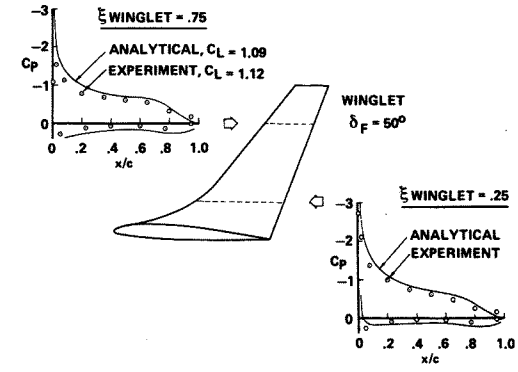

Figure 10 Comparison of Analytical and Experimental Winglet Pressures

The reduction in induced drag due to winglets at flap deflections representative of takeoff and landing conditions is shown in Fig. 11. Results obtained by two analytical methods are compared to experimental results in this figure. The induced drag values for the lower curve were calculated by Trefftz plane analysis of the span load obtained from the panel method. Induced drag depicted by the upper curve were calculated from the vortex lattice program. At lift coefficient values where the flow is still attached, the theoretical results agree well with experiment. The agreement tapers off at the higher lift coefficients as flow separation on the wing and winglet progressively worsens. Whenever viscous effects dominate, the magnitude of the drag reduction was not accurately predicted. Nevertheless, the trend was correctly calculated.

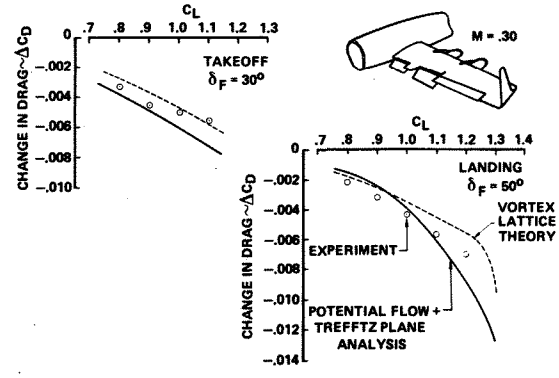

Figure 11 Low Speed Predictions for KC-135A with Winglets

Nacelle Installation Analysis

Trends in advanced engine technology are toward higher bypass ratios, mixed flow exhausts, and quieter nacelle designs. To integrate these larger diameter, longer cowls to the airframe, without introducing substantial penalties in structural weight and interference drag, requires careful tailoring of the nacelle, strut, and airframe. The subsonic, inviscid panel methods have been applied to underwing pylon-mounted naceles to determine the sources of drag of such installations, and to define nacelle and strut shapes that reduce the pylon-nacelle interference drag.[21] The capability of the panel methods to provide a detailed definition of surface pressure data, as well as flow field data, necessary for the understanding of such difficult flow problems is illustrated in Fig. 12. To obtain the same type of information by wind tunnel testing would require an extremely dense array of static pressure taps. The cost of such testing would be prohibitive. The detailed flow

information obtained by the isobar patterns shown in Fig. 12 is extremely useful for diagnosing the design for possible flow problems, for providing loads data information, and for indicating flow field characteristics for evaluating the impact on engine performance.

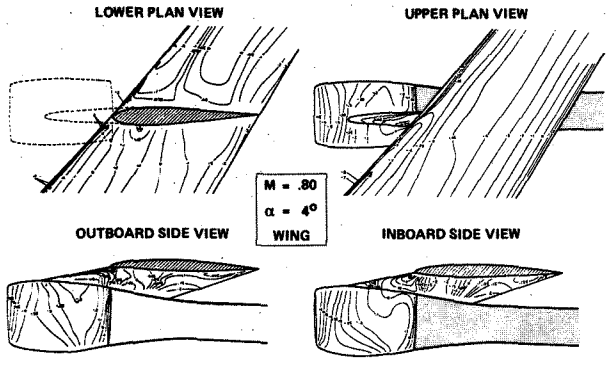

Figure 12 Calculated Isobars for Outboard Engine Installation on B747

A procedure was devised to use the axisymmetric transonic jet plume program in such a way that the effect of the pylon bifurcator in the fan exhaust could be predicted. The three-dimensional plume shape resulting from this procedure can then be used in the three-dimensional panel method. Typical results comparing calculated and experimental nacelle pressure using this technique are shown in Fig. 13. The excellent agreement exhibited in this figure is representative of underwing pylon-mounted nacelles where transonic local flow and viscous effects are small.

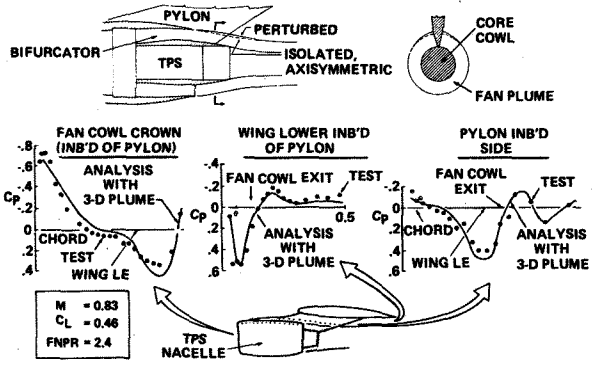

Figure 13 Comparison of Analysis with Three-Dimensional Plume To Test for Installed Power Nacelle

Emphasis has been placed on analytically determining the interference drag on current transport type configurations. Installation of an advanced technology engine on the B747-200 was selected to validate the accuracy and applicability of the method. The most significant finding was that engine installation drag was predicted well by the analysis, and that most of the interference drag is due to the distortion in the spanload distribution caused by the induced flow field created by the nacelle on the wing. The effect of the outboard engine installation on the B747 obtained by theory is compared to the calculated spanload obtained by experiment in Fig. 14. The significant loss in lift due to the outboard nacelle installation is well predicted by theory. The comparison of the nacelle increment drag obtained by analysis and by testing for three different nacelle-strut installations is shown on the right-hand side of Fig. 14. The analysis data falls well within the accuracy of

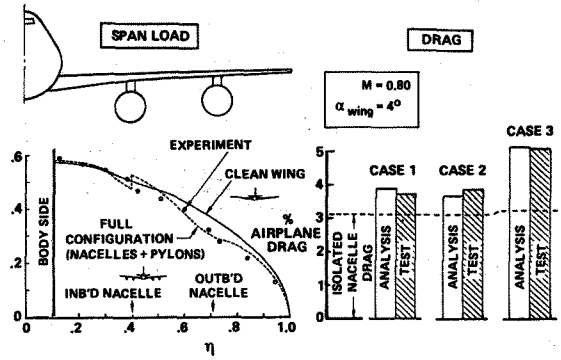

Figure 14 Analysis of B747 SP Wing Loading and Nacelle Drag

the experimental data. The drag increment due to the nacelle includes both profile drag and induced drag calculations. Profile drag was calculated by using the surface pressures calculated by the panel method as inputs to a two-dimensional boundary layer program. Induced drag was calculated by using the spanload obtained by the panel method as input to the Trefftz plane analysis method. It is important to note, that the majority of the nacelle interference drag (nacelle drag increment minus profile drag) resulted from the change in span loading. Once the major cause of nacelle interference drag was identified, the approach became to design, by analysis, a nacelle that would not have a detrimental effect on wing spanload and thus reduce the induced drag. The aim was to shape the nacelle in such a manner that when placed under the wing, it would not create a distortion in the basic wing-body configuration spanload. The vortex lattice program was used to analyze nacelle position and orientation. The results of the analysis indicated that by tilting the axisymmetric nacelle down by 6°, no load would be induced on the wing (see Fig. 15). Since this was an impractical solution, an alternative approach was to shape the nacelle such that at 0° tilt it would generate the same negative nacelle lift as the axisymmetric nacelle at 6° tilt down. Through an iterative process, using the vortex lattice program, the nacelle shape shown in Fig. 15 was selected. This nacelle does not distort the span load and, thus, greatly reduces the interference drag due to the engine installation. Analysis also indicates that favorable interference due to the nacelle can be realized by cambering the nacelle strut to generate an outboard load in a manner analogous to a winglet.

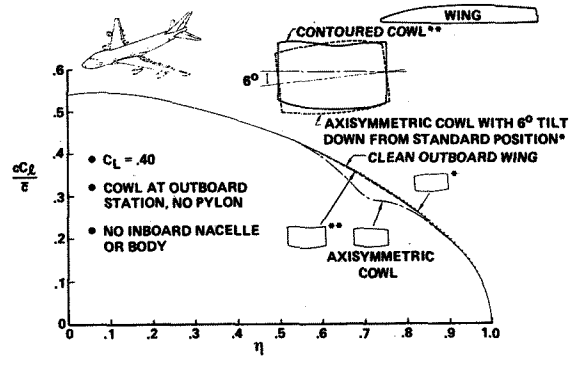

Figure 15 Effect of Cowl Shape on B747 Wing Loading

The nacelle shaping concept has been applied to the design integration of a new advanced technology engine to the B707-320 airplane. The new engine is very large in diameter, must be mounted close to the wing for ground clearance, and has a long duct that places the fan cowl very close to the leading edge of the

wing. The top right-hand side of Fig. 16 shows the geometry comparison between the original nacelle and the new advanced technology nacelle. Force data shown at the bottom left-hand side of Fig. 16 shows that the new nacelle incurs a smaller interference and blowing drag than the original.

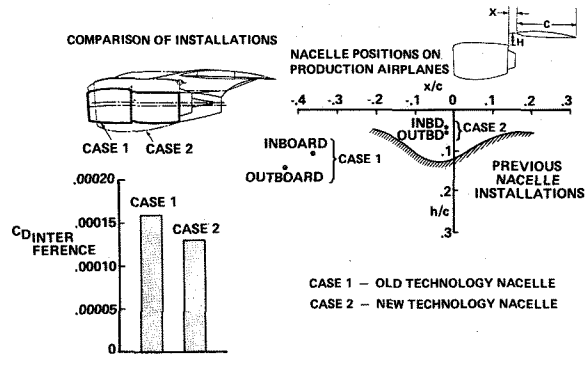

Figure 16 Nacelle Installations

This successful nacelle integration could not have been achieved using previous design techniques, which rely heavily upon past trends of aircraft. For example, the right side of Fig. 16 shows the established trend of nacelle placement with respect to the wing that achieves minimum nacelle integration drag. Since data for successful transport aircraft fall below the trend line, positioning a nacelle above this line would have suggested that a large drag penalty would have been incurred. However, the analysis allowed development of a satisfactory design.

Transonic Wing Analysis

The validation of three-dimensional transonic potential flow methods has been reported recently in several papers, e.g., see References 22, 23, 24, and 25, to name a few. During the application of the finite volume transonic method at Boeing, it was found that the number of iterations used to solve the finite difference equations had a more pronounced influence on the accuracy of the solution than had been previously estimated. Since the number of cumulative iterations used within the program is proportional to the cost required to perform an analysis, the number has been generally limited to 100, as recommended in Reference 10. However, the number of iterations used to complete a solution has a dramatic influence on the resulting wing chordwise pressure distributions and on the spanwise lift, drag, and pitching moment distributions. An example of this effect on the wing chordwise pressure distribution is shown in Fig. 17. The analysis was done for a free-stream Mach number of 0.84 and a wing lift coefficient of 0.53. Although the wing's lower surface pressures change only slightly while iterations increased from 50 to 400, the upper surface pressures vary significantly, especially in the region of the shock. The solution is apparently converging, since the changes in the pressure distributions diminish with increasing iteration number.

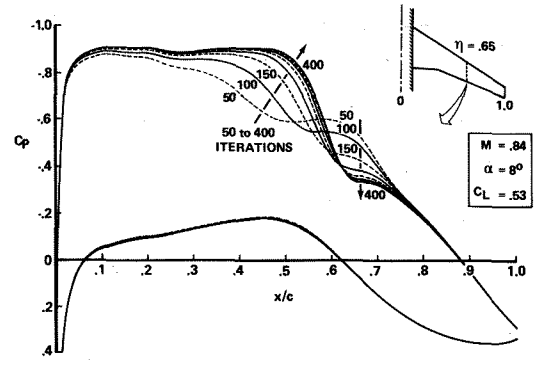

Figure 17 Effect of Iterations on Chordwise Pressure Distribution Calculated using the Three-Dimensional Transonic Potential Flow Method.

The viscous displacement effect of the three-dimensional boundary layer over the wing surface must be taken into account in order to produce accurate performance characteristics. The coupling of the three-dimensional boundary layer method[15] with inviscid potential flow programs provides the capability for better wing design, for diagnosis of specific wing design problems, and for evaluating the wing performance beyond the Reynolds number range of present wind tunnels. An interface program was developed that supplies grid geometry and outer flow boundary conditions inputs to the boundary layer program. The outer flow description is obtained either from the three-dimensional transonic flow method[10] or from the panel aerodynamics method.[1] Another interface program interpolates the boundary layer results back to the potential flow grid, and thereby, it is possible to cycle several times between viscous and inviscid programs. The major interfaces between these methods are illustrated in Fig. 18.

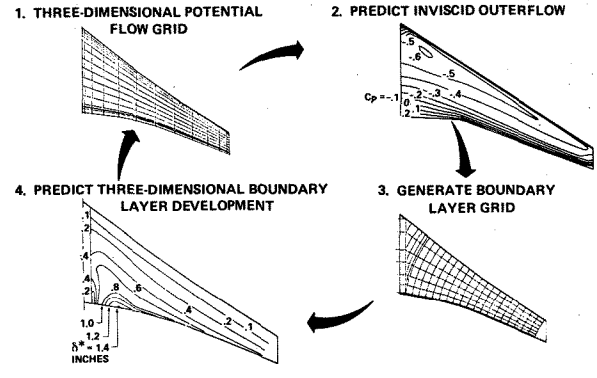

Figure 18 Illustration of Major Interfaces Involved in the Calculation of Three-Dimensional Boundary Layers on Wings

The coupled boundary layer-potential flow method was initially validated by a comparison with boundary layer measurements on a 45° swept wing of constant chord, and aspect ratio, AR, of 5.[26] The upper portion of Fig. 19 shows the location on the planform of the boundary layer profile measurement stations. The potential flow was analyzed using the subsonic panel method.

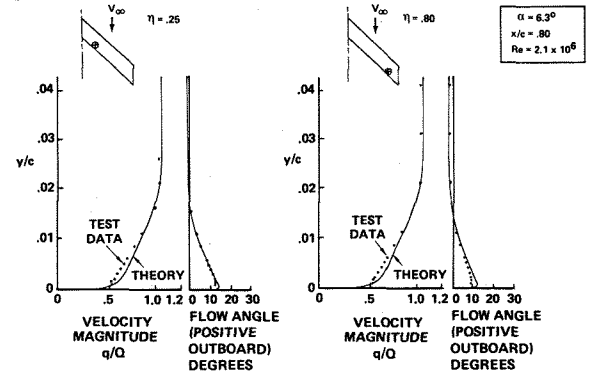

Figure 19 Three-Dimensional Boundary Layer Correlations

Velocity profile comparisons are shown in the lower portion of Fig. 19 for inboard and outboard stations at 80% chord and for an angle-of-attack, α, of 6.3°. The small disagreement at the outer edge of the layer represents the discrepancy between the potential flow analysis and the measured outer flow. Note that the velocity magnitudes are normalized by the far-field value, and thus, they do not approach 1.0 with increasing height. Within the layer, the agreement is good, considering the limitations of the eddy viscosity model at such low Reynolds number, viz., $Re \approx 2.1 \times 10^6$. This was one of the first test cases used to validate the method, and only one inviscid-viscous cycle was conducted. Additionally, the location of the boundary layer transition was not reported precisely for the experiment and had to be assumed for the analysis.

It has been found that a number of cycles between the transonic potential flow program and the boundary layer program is necessary to achieve a satisfactory converged solution, i.e., until the pressure distribution and the boundary layer displacement thickness, δ^*, do not change significantly between cycles. Also, as the cumulative number of iterations within the transonic program increases, the shock wave pattern becomes better defined. As the shock wave sharpens up, it becomes necessary to run the boundary layer analysis often enough so that it can react along with the changing pressure distribution. The effect of the number of iteration cycles on the chordwise pressure distribution and displacement thickness is shown on Fig. 20. Shock location and the predicted boundary layer separation line are also shown in this figure.

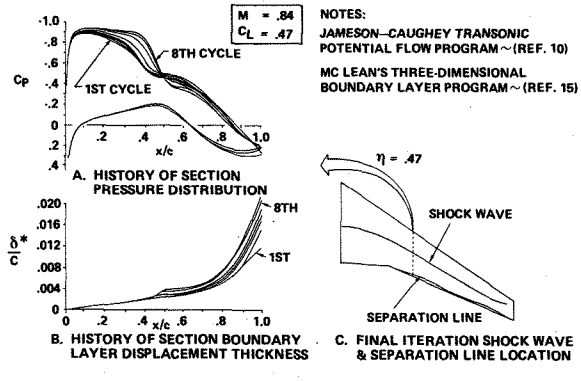

Figure 20 Typical Results of Three-Dimensional Transonic Potential Flow/ Three-Dimensional Boundary Layer Interactive Procedure

A comparison of pressures calculated by the coupled viscous-inviscid method to those obtained from wind tunnel testing of an advance technology wing are shown in Fig. 21. The general trends of the measured pressure distributions are matched by the theory. However, the lower surface pressure level is surprisingly not well predicted. This apparent shift in lower surface pressure level has not been reported by others, and the cause for this level shift is unknown at this time. In addition, the sections near the side of the body show higher surface velocities for the test data compared to predictions. This may be due to high velocities induced on the wing by the presence of the body. The cylindrical body option of the transonic potential flow method has not yet been satisfactorily checked out, and consequently, it is not utilized. A simple reflection plane is assumed at the side of the body, which, of course, does not account for the presence of the body at all.

The test-theory comparison of spanwise lift and moment distribution at Mach of 0.84 is portrayed in Fig. 22 for the same advanced technology wing mentioned above. The shape comparison for the lift distribution appears good, however, the theoretical level is high due mainly to the lack of correlation on the lower surface pressures. The pitching moment distribution comparison shows good correlation between theory and experiment.

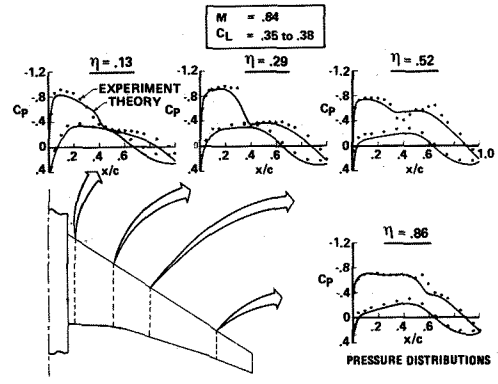

Figure 21 Comparison of Experimental and Theoretical Pressure Distributions

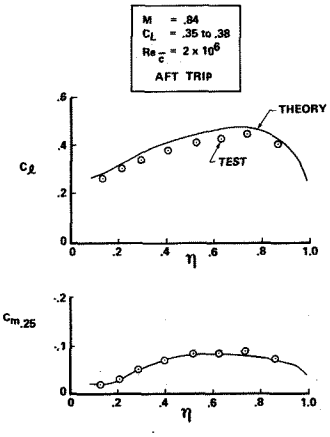

Figure 22 Section Lift and Moment Test-Theory Comparison, M = .84

The test-theory comparisons for the spanwise integrated values of wave and profile drag and for the spanwise variation of profile drag are depicted in Fig. 23. Profile drag was calculated by applying the Squire-Young formula [27] along the wing trailing edge. Only the streamwise components of the trailing edge velocity profiles are used in this formulation. Wave drag was calculated from the transonic potential flow program; measured wave drag was obtained by extracting the wave drag contribution from wake profiles measured in the wind tunnel, e.g., see Fig. 24. Measured and calculated profile and wave drags compare reasonably well as indicated in Fig. 23. The capability of estimating the spanwise variation of wing drag components, as presented above, identifies the critical wing design regions and allows for proper wing modification with reasonable assurance of success.

The drag polar comparison between wind tunnel measured lift and drag and that calculated by the coupled viscous-inviscid method is shown in Fig. 25 for Mach numbers of 0.70 and 0.84. Results were calculated for three angles-of-attack for each Mach condition. A constant drag increment was added to the theoretical data as an estimation for body and model mounting system effects. The comparison shows that the general trends of the test curves are predicted by the theory, however, exact agreement is not obtained, since the fuselage could not be included in the theoretical model.

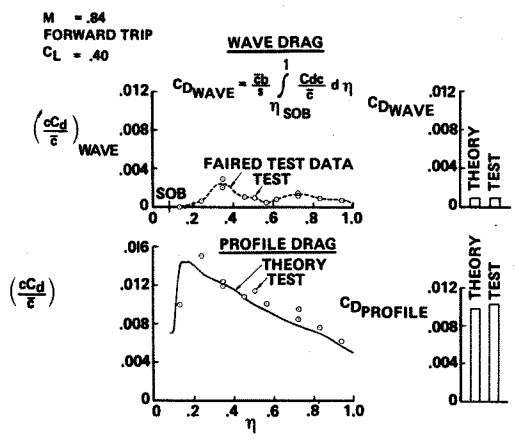

Figure 23 Spanwise Profile and Wave Drag Distributions, M = .84

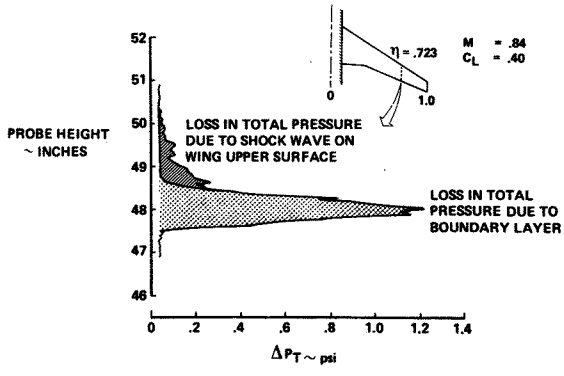

Figure 24 Wake Profile Measurement

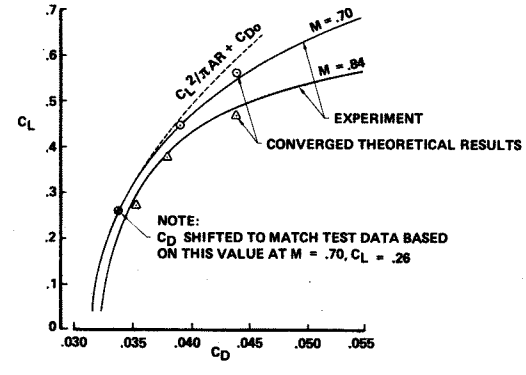

Figure 25 Comparison of Converged Theoretical and Experimental Drag Polars

IV. Concluding Remarks

The significant advances that have been made in computational fluid mechanics are having considerable impact on the aerodynamic design process. Subsonic panel methods, when used within their limits of application, provide valuable insight into complex flow fields, guidance for achieving integrated designs, and ability to explore innovative configuration designs. The use of these methods can substantially increase airplane performance capabilities. The integrated computer program system to analyze transonic, viscous flows over transport type wings has emerged as a very important tool to support the wing design process, and to support diagnostic investigation of the wing performance.

Rewarding as the accomplishments in computational aerodynamic design have been, much work remains yet to be done. In the panel methods, work is underway at Boeing in the Panel Aerodynamics System (PAN AIR). This will greatly simplify the user's imput and output data manipulation and reduce computer costs. The three-dimensional transonic potential flow methods need to be expanded to include the complete configuration. The three-dimensional boundary layer method needs to be enhanced to incude the fuselage, to account properly for shock-boundary layer interaction, to include the interaction effects associated with the viscous flow in the region of the trailing edge and near wake, to handle surface intersection problems, and to analyze separated flows.

The coupled three-dimensional transonic viscous-inviscid method has emerged as the most significant tool for the analysis of transport wings at transonic flow conditions. However, this integrated system of computer programs is only operational within the applied research environment and not in the project engineering area, since considerable skill must be developed by the users. The vast amount of data evaluation and transfer between the various component programs precludes new users from becoming suitably proficient in its operation in a short period of time. Moreover, the entire process is severely hampered by the excessive flow time (time from initiation to completion) and high computational cost of completing an analysis. For example, the advanced technology wing discussed herein was designed (using subcritical analysis methods and inhouse wing design procedures), a model was built that incorporated eight rows of static pressure taps, and a wind tunnel test was completed that included the measurement of forces, pressures, and wake rake data in a shorter time period and at approximately the same cost as it took to obtain the analytical data. From the design engineer's point of view, the easy preparation of input data, the visibility of output, and the flow time required to obtain the final results are just as important as the algorithms used to calculate the numbers. Furthermore, the extremely high cost of running these new methods limits their usability to complement and enhance the results obtained experimentally.

The long flow time and high computer costs of the new methods need significant improvements if these methods are to be used in the engineering environment to support and guide the evolutionary design process in a timely manner. If these enhancements are not included in these methods, we may never experience a reduced reliance on the wind tunnel in airplane design as many computer experts suggest. Instead, these new analytical capabilities will be continually relegated to the applied research environment rather than the project engineering area.

Acknowledgement

The author wishes to acknowledge the contributions of the many individuals within The Boeing Company who conducted many of the analyses reviewed in this paper. Appreciation is extended to the United States Air Force Flight Dynamics Laboratory, Aeromechanics Division, for their support of the KC-135 winglet study. Additional thanks are due to the National Aeronautics and Space Administration, Lyndon B. Johnson Space Center, for their funding of the analysis of the B747 Space Shuttle Carrier Aircraft.

References

1. Rubbert, P.E., and Saaris, G.R., "Review and Evaluation of a Three-Dimensional Lifting Potential Flow Analysis Method for Arbitrary Configurations," AIAA Paper No. 72-188, AIAA 10th Aerospace Sciences Meeting, San Diego, Calif., January 17 - 19, 1972.
2. Rubbert, P.E., and Saaris, G.R., "A General Three-Dimensional Potential-Flow Method Applied to V/STOL Aerodynamics," SAE Journal, Vol. 77, Sept. 1969.
3. Johnson, F.T., "A General Panel Method for the Analysis and Design of Arbitrary Configurations in Subsonic Flows," Document No. D6-43808, Feb. 1976, The Boeing Company, Seattle, Wash.
4. Feifel, W.M., "Optimization and Design of Three-Dimensional Aerodynamic Configurations of Arbitrary Shape by a Vortex Lattice Method," NASA SP-405, Proceedings of NASA-Langley Vortex Lattice Work Shop, May 17-18, 1976, pp. 71-88, Washington, D.C.
5. Ashley, H., and Landahl, M.T., Aerodynamics of Wings and Bodies, Addison-Wesley Publishing Co., Inc., Reading, Mass., 1965.
6. Lundry, J.L., "Calculation of Lift and Induced Drag from Sparse Span Loading Data," Journal of Aircraft, Vol. 14, No. 3, Mar. 1977, pp. 309-311.
7. Brown, S., "Trefftz Plane Calculation of Induced Drag," unreleased document, The Boeing Company, Seattle, Wash.
8. Ehlers, F.E., "A Numerical Method for Computing the Transonic Fan Duct Flow Over a Centerbody into an Exterior Free Stream - Program TEA-343," Document No. D6-41078, Sept. 1974, The Boeing Company, Seattle, Wash.
9. Caughey, D.A., and Jameson, A., "Numerical Calculation of Transonic Potential Flow about Wing-Fuselage Combinations," AIAA Paper No. 77-677, AIAA 3rd Computational Fluid Dynamics Conference, Albuquerque, N.Mex., June 27-28, 1977.
10. Jameson, A., and Caughey, D.A., "A Finite Volume Method for Transonic Potential Flow Calculations," AIAA Paper No. 77-635, AIAA 3rd Computational Fluid Dynamics Conference, Albuquerque, N.Mex., June 27-28, 1977.
11. Bailey, F.R., and Ballhaus, W.F., "Comparisons of Computed and Experimental Pressures for Transonic Flows About Isolated Wings and Wing-Fuselage Combinations," NASA SP-347, March 1975, pp. 1213-1231, Washington, D.C.
12. Boppe, C.W., "Computational Transonic Flow About Realistic Aircraft Configurations," AIAA Paper No 78-104, AIAA 16th Aerospace Sciences Meeting, Huntsville, Ala., Jan. 16-18, 1978.
13. Schmidt, W., and Vanino, R., "The Analysis of Arbitrary Wing-Body Combinations in Transonic Flow Using a Relaxation Method," Symposium Transonicum II, Springer-Verlag, Berlin, 1976, pp. 523-532.
14. Chen, A., Tinoco, E., and Yoshihara, H., "Transonic Computational Design Modifications of the F-111 TACT," AIAA Paper No. 78-106, AIAA 16th Aerospace Sciences Meeting, Huntsville, Ala., Jan. 16-18, 1978.
15. McLean, J.D., "Three-Dimensional Turbulent Boundary Layer Calculations for Swept Wings," AIAA Paper No. 77-3, AIAA 15th Aerospace Sciences Meetings, Los Angeles, Calif., Jan. 1977.
16. Boctor, M., "747-Orbiter Piggy-Back Configuration Potential Flow Analysis," unreleased document, The Boeing Company, Seattle, Wash.
17. Whitcomb, R.T., "A Design Approach and Selected Wind-Tunnel Results at High Subsonic Speeds for Wing-Tip Mounted Winglets," NASA TN D-8620, 1976, Washington, D.C.
18. Flechner, S.G., Jacobs, P.F., and Whitcomb, R.T., "A High Subsonic Speed Wind-Tunnel Investigation of Winglets on a Representative Second Generation Jet Transport Wing," NASA TN D-8264, 1976, Washington, D.C.
19. Montoya, L.C., Flechner, S.G., and Jacobs, P.F., "Effect of Winglets on a First-Generation Jet Transport Wing. II - Pressure and Spanwise Load Distributions for a Semi-Span Model at High Subsonic Speeds," NASA TN D-8474, 1977, Washington, D.C.
20. Ishimitsu, K.K., "Aerodynamic Design and Analysis of Winglets," AIAA Paper No. 76-940, AIAA Aircraft Systems and Technology Meeting, Dallas, Tex., Sept. 27-29, 1976.
21. Gillette, W.B., "Nacelle Installation Analysis for Subsonic Transport Aircraft," AIAA Paper No. 77-102, AIAA 15th Aerospace Sciences Meeting, Los Angeles, Calif., Jan. 24-26, 1977.
22. Gustavsson, A.L., and Hedman, S.G., "Design and Test of a Sonic Roof-Top Pressure Distribution Wing," Symposium Transonicum II, Springer-Verlag, Berlin, 1976, pp. 273-280.
23. Vanino, R., and Rohlfs, S., "Supercritical Wing Design for a Fighter Type Experimental Aircraft," Symposium Transonicum II, Springer-Verlag, Berlin, 1976, pp. 281-288.
24. Haney, H.P., Waggoner, E.G., and Ballhaus, W.F., "Computational Transonic Wing Optimization and Wind Tunnel Test of a Semi-Span Wing Model," AIAA Paper No. 78-102, AIAA 16th Aerospace Sciences Meeting, Huntsville, Ala., Jan. 16-18, 1978.
25. Henne, P.A., and Hicks, R.M., "Transonic Wing Analysis Using Advanced Computational Methods," AIAA Paper No. 78-105, AIAA 16th Aerospace Sciences Meeting, Huntsville, Ala., Jan. 16-18, 1978.
26. Brebner, G.G., and Wyatt, L.A., "Boundary Layer Measurements at Low Speed on Two Wings of 45° and 55° Sweep," Aeronautical Research Council, C.P. No. 554, 1961.
27. Squire, H.B., and Young, A.D., "The Calculation of the Profile Drag of Aerofoils," Aeronautical Research Committee, Reports and Memoranda No. 1838, Nov. 18, 1937, London.